



Rezaei *et al.*, 2020] account for explainability, but they cannot provide faithful explainability as they rely on post hoc model-agnostic explainability [Rudin, 2019]. With the above constraints in mind, we therefore propose a lightweight, efficient and explainable-by-design CNN for traffic classification, and evaluate it on a large-scale commercial-grade dataset.

The contributions of this paper are the following:

- We present a new Lightweight, Efficient and eXplainable-by-design CNN (LEXNet) for encrypted traffic classification, which relies on a new residual block and prototype layer;
- Based on a commercial-grade dataset, we show that LEXNet is more accurate than the current state-of-the-art explainable-by-design CNN (ProtoPNet [Chen *et al.*, 2019]), and maintains the same accuracy as the best performing deep learning approach (ResNet [He *et al.*, 2016]) that does not provide faithful explanations;
- We demonstrate that LEXNet significantly reduces the model size and inference time compared to the current state-of-the-art neural networks with explainability-by-design and post hoc explainability methods;
- We illustrate the explainability of our approach which stems from the communication of detected application/class prototypes to the end-user. Moreover, we highlight the faithfulness of LEXNet explanations by comparing them to the ones provided by state-of-the-art post hoc explainability methods.

## 2 Related Work

Traffic classification can be formulated as a Multivariate Time Series (MTS) classification task, where the input is packet-level data (e.g., packet size, direction) related to a single flow<sup>1</sup>, and the output is an application label. The state-of-the-art approaches [Aceto *et al.*, 2019a; Beliard *et al.*, 2020; Liu *et al.*, 2019; Lotfollahi *et al.*, 2020; Nascita *et al.*, 2021; Rezaei *et al.*, 2020; Wang *et al.*, 2020] adopt heavyweight deep learning classifiers (from 1M to 2M weights), and do not discuss the impact of their model size on the accuracy and inference time. When accounting for explainability, these studies employ post hoc explainability methods like SHAP [Lundberg and Lee, 2017], which cannot meet the faithfulness requirements. Finally, the results of these studies are not directly comparable as they are evaluated on different datasets. Plus, these datasets (mostly private, from 8 to 80 applications and from 8k to 950k flows) fail to reflect the diversity of applications in real commercial settings.

Consequently, an accurate, lightweight, efficient and explainable-by-design approach for traffic classification evaluated on a public commercial-grade dataset is necessary. We identified CNNs as having the potential to fulfill these needs. In the next sections, we present the corresponding machine learning state-of-the-art (MTS classification, explainability,

<sup>1</sup>A packet is a unit of data routed on the network, and a flow is a set of packets that shares the same 5-tuple (i.e. source IP, source port, destination IP, destination port, and transport-layer protocol) [Valenti *et al.*, 2013].

lightweight and efficient architectures) on which we position our approach.

### 2.1 MTS Classification

The state-of-the-art MTS classifiers are composed of three categories: similarity-based [Seto *et al.*, 2015], feature-based [Baydogan and Rungar, 2016; Karlsson *et al.*, 2016; Schäfer and Leser, 2017; Tuncel and Baydogan, 2018] and deep learning methods [Karim *et al.*, 2019; Zhang *et al.*, 2020; Fauvel *et al.*, 2021]. The results published show that the top two most accurate MTS classifiers on average on the public UEA archive [Bagnall *et al.*, 2018] are deep learning methods (top-1 XCM [Fauvel *et al.*, 2021], top-2 MLSTM-FCN [Karim *et al.*, 2019]). XCM extracts discriminative features related to observed variables and time directly from the input data using 2D and 1D convolutions filters, while MLSTM-FCN stacks a LSTM layer and a 1D CNN layer along with squeeze-and-excitation blocks to generate latent features. Therefore, in this work, we choose to benchmark our LEXNet to these two MTS classifiers. Plus, we integrate in our benchmark the commonly adopted state-of-the-art CNNs in computer vision (ResNet [He *et al.*, 2016], DenseNet [Huang *et al.*, 2017]), the vanilla 1D CNN widely used in traffic classification studies, and the traditional machine learning methods Random Forest [Breiman, 2001] and XGBoost [Chen and Guestrin, 2016].

### 2.2 Explainability

There are several methods belonging two main categories [Du *et al.*, 2020]: explainability-by-design and post hoc explainability.

Post hoc methods are the most popular ones for deep learning models (e.g., the saliency method Grad-CAM [Selvaraju *et al.*, 2017], the surrogate model SHAP [Lundberg and Lee, 2017]). However, some recent studies [Rudin, 2019; Chen *et al.*, 2020] show that post hoc explainability methods face a faithfulness issue.

Lately, there have been some work proposing explainability-by-design CNN approaches [Zhang *et al.*, 2018; Chen *et al.*, 2019; Elsayed *et al.*, 2019; Chen *et al.*, 2020] to circumvent this issue. Two of these approaches [Zhang *et al.*, 2018; Elsayed *et al.*, 2019] provide the explainability-by-design feature but at the cost of some lag behind the state-of-the-art CNNs in terms of accuracy, which remains a prerequisite for our task. Then, Chen et al. (2020) present Concept Whitening, an alternative to a batch normalization layer which decorrelates the latent space and aligns its axes with known concepts of interest. This approach requires that the concepts/applications are completely decorrelated, so it is not suited for our traffic classification task as some applications can be correlated (e.g., different applications from the same editor). Finally, another approach combines accuracy with explainability-by-design: ProtoPNet [Chen *et al.*, 2019]. It consists of a CNN backbone to extract discriminative features, then a prototype block that computes similarities to the learned class-specific prototypes as basis for classification. This approach is particularly interesting for our task as the prototype explanations can be used to form application signatures for network experts. Therefore, with the objective

to combine accuracy and explainability-by-design suited for traffic classification, we adopted a prototype-based CNN approach. Then, we worked to reduce the number of weights and inference time of the approach while maintaining the accuracy, in particular with regard to the CNN backbone.

### 2.3 Lightweight and Efficient Architectures

Multiple studies about lightweight and efficient CNN architectures have been published over the last years: ShuffleNetV2 [Ma *et al.*, 2018] and its four practical guidelines, EfficientNet [Tan and Le, 2019] with its scaling method along depth/width/resolution dimensions, MobileNetV3 [Howard *et al.*, 2019] with its network search techniques and optimized nonlinearities, GhostNet [Han *et al.*, 2020] using a Ghost module based on linear transformations, and CondenseNetV2 [Yang *et al.*, 2021b] relying on a Sparse Feature Reactivation module.

These CNNs are evaluated on the same public dataset (ImageNet). However, most of these evaluations optimize a proxy metric to measure efficiency (number of floating-point operations, FLOPs), which is not always equivalent to the direct metric we care about - the inference time [Ma *et al.*, 2018]. Using FLOPs as the reference, these studies do not evaluate the accuracy and inference time on a comparable model size (number of weights). A recent work [Ridnik *et al.*, 2021] shows that ResNet architecture is usually faster than its latest competitors, offering a better accuracy/inference time trade-off (which is also confirmed by our experiments in Section 5.1). Therefore, we adopted ResNet as CNN backbone and revisited its residual block to make it lighter and more efficient. We include ShuffleNetV2, EfficientNet, MobileNetV3, GhostNet and CondenseNetV2 in our benchmark, and perform a comparison of the accuracy and inference time based on a comparable model size in Section 5.1.

## 3 Algorithm

We now propose our new Lightweight, Efficient and eXplainable-by-design CNN classifier (LEXNet). First, we present ProtoPNet [Chen *et al.*, 2019], the starting point of LEXNet. Then, we explain how LEXNet, with the introduction of a new residual block and prototype layer, reduces the number of weights and inference time of this network, while preserving the explainability-by-design. Our evaluation in Section 5 shows that LEXNet also outperforms ProtoPNet in terms of accuracy.

### 3.1 ProtoPNet

ProtoPNet integrates in its design a form of explainability that agrees with the way humans describe their own thinking in classification tasks: it focuses on parts of the input data and compares them with prototypical parts of the data from a given class (illustrated in Section 5.2). The network consists of a regular CNN as backbone, followed by a prototype block and a fully connected layer. Given an input sample, the convolutional layers of the model extract useful features for prediction. Then, the prototype block learns class-specific prototypes, with the number and size of prototypes per class set as hyperparameters of the algorithm. The left side of Figure 1 illustrates the prototype block of ProtoPNet with the

hyperparameter setting of our experiments (detailed in Section 5): two prototypes of size  $(1, 1)$  per class with 200 classes in the dataset. Each prototype in the block (e.g., size of each prototype in Figure 1:  $1 \times 1 \times 128$ ) computes the L2 distances with all patches of the last convolutional layer (e.g., size of the last layer in Figure 1:  $20 \times 2 \times 128$ ), and inverts the distances into similarity scores. The result is an activation map of similarity scores (e.g., size of a similarity matrix in Figure 1:  $20 \times 2$ ). This activation map preserves the spatial relation of the convolutional output, and can be upsampled to the size of the input sample to produce a heatmap that identifies the part of the input sample most similar to the learned prototype. To make sure that the learned class-specific prototypes correspond to training samples patches, the prototypes are projected onto the nearest latent training patch from the same class during the training of the model. The activation map of similarity scores produced by each prototype is then reduced using global max pooling to a single similarity score, which indicates how strong the presence of a prototypical part is in some patch of the input sample. Finally, the classification is performed with a fully connected layer based on these similarity scores.

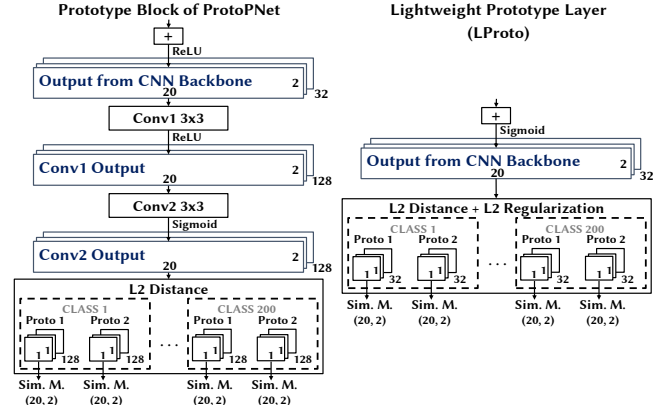


Figure 1: The prototype block of ProtoPNet and the new lightweight prototype layer of LEXNet. Sim. M. - similarity matrix.

### 3.2 LEXNet

LEXNet relies on the same pipeline as ProtoPNet: a CNN backbone for feature extraction, a prototype block for explainability-by-design, and a fully connected layer for classification. We select ResNet [He *et al.*, 2016] for the CNN backbone as it obtains the best accuracy on our traffic classification dataset (see results in Section 5.1). However, ResNet exhibits only the second best inference time, an aspect which is critical for our application. Therefore, our first contribution is to introduce a new lightweight and efficient residual block which reduces the number of weights and inference time of the original residual block, while preserving the accuracy of ResNet. To further reduce the size of LEXNet and improve its accuracy, we propose as a second contribution to replace the prototype block of ProtoPNet with a new lightweight prototype layer. We present in the next sections these two contributions, and end with the overall architecture of our network.

## Lightweight and Efficient Residual Block

ResNet is a state-of-the-art CNN. It is composed of consecutive residual blocks which consist of two convolutions with a shortcut added to link the output of a block to its input in order to reduce the vanishing gradient effect [Zagoruyko and Komodakis, 2016]. When the number of output channels equals the one of the input channels, the input data is directly added to the output of the block with the shortcut. Nonetheless, the prediction performance of ResNet is supported by an increase in the number of channels along the depth of the network to learn elaborated features, which implies residual blocks with a higher number (usually twice) of output channels than input channels. In this case, before performing the addition, another convolution is applied to the input data in order to match the dimensions of the block output. A residual block is illustrated on the left side of Figure 2 with  $n$  input channels and  $2n$  output channels. We can see in this Figure that two convolutions have a different number of output channels than input channels (Convolutions 1 and 3). However, a guideline from [Ma *et al.*, 2018] (ShuffleNetV2) states that efficient convolutions should keep an equal channel width to minimize memory access cost and inference time. Therefore, we propose a new residual block that only performs convolutions with an equal channel width, and the additional feature maps are generated with two cheap operations (see block on the right side of Figure 2).

First, the authors of GhostNet [Han *et al.*, 2020] state that CNNs with good prediction performance have redundancy in feature maps, and that substituting some of the feature maps with a linear transformation of the same convolution output does not impact the prediction performance of the network. Therefore, we double the number of feature maps from the first convolution in a cost-efficient way using a series of linear transformations of its output ( $3 \times 3$  linear kernel). These new feature maps are concatenated to the ones from the first convolution output to form the input of the second convolution<sup>2</sup>. Thus, the first and second convolutions in our new residual block have an equal channel width ( $n$  and  $2n$  respectively, see Figure 2).

The second operation concerns the shortcut link: instead of converting the input data to the block output dimensions with a third convolution (see Res block in Figure 2), we propose to save this convolution by keeping the input data and concatenating it with the output from the first convolution. Our experiments on the traffic classification dataset show that the new residual block LERes allows ResNet to reduce the number of weights of the backbone by 19.1% and the CPU inference time by 41.3% compared to ResNet with the original residual block, while maintaining its accuracy (99.3% of the original accuracy).

<sup>2</sup>We have also considered having both convolutions 1 and 2 with an equal channel width  $n$ , and moving the concatenate operation with the feature maps from the linear transformation after the convolution 2. However, our experiments showed that this configuration leads to a decrease in accuracy without noticeable drop in inference time.

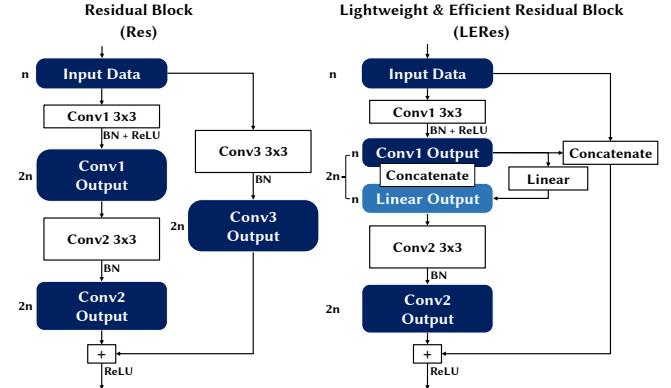


Figure 2: ResNet original residual block and our new lightweight and efficient residual block.

## Lightweight Prototype Layer

Next, we adopt a new lightweight prototype layer instead of the prototype block of ProtoPNet. As illustrated in Figure 1, the prototype block of ProtoPNet adds two convolutional layers with an important number of channels to the CNN backbone (recommended setting:  $\geq 128$ ). Then, it connects the prototype layer with a Sigmoid activation function. Finally, the prototypes have the same depth as the last convolutional layer (e.g., 128) for the computation of the similarity matrices with the L2 distance. We propose to remove the two additional convolutional layers (see right block of Figure 1). As a consequence, the prototypes have a much smaller depth (same as CNN backbone output: 32 versus 128). Thus, our new prototype layer allows us to reduce the number of weights by 29.4% compared to the original prototype block of ProtoPNet, and implies a 17.0% reduction in CPU inference time - see details in Section 5.1. Then, we replace the last activation function from the CNN backbone with a Sigmoid. As suggested in [Sandler *et al.*, 2018] and confirmed by our experiments (see Section 5.1), replacing the ReLU activation function from the last layer of our CNN backbone with a Sigmoid improve the accuracy of our network. Finally, we further improve the accuracy of our network by adding an L2 regularization on the weights of the prototypes in order to enhance its generalization ability. Considering the limited number of prototypes, and supported by the results from our experiments, we have selected an L2 regularization over an L1 sparse solution.

## Network Architecture

The overall architecture of LEXNet is presented in Table 1. In order to limit the size of our network, the number of LERes blocks has been determined by cross-validation on the training set. Thus, additional LERes blocks would not increase the accuracy of the network on our traffic classification dataset. A higher number of filters would not increase the accuracy either. Concerning the explanations supporting network predictions, as presented in Section 3.1, activation maps from the prototype layer can be upsampled to the size of the input sample to produce a heatmap that identifies the part of the input sample most similar to the learned prototype. It has been shown in [Fauvel *et al.*, 2021] that applying upsampling

processes to match the size of the input sample can affect the precision of the explanations. Therefore, we keep the feature map dimensions over the network the same as the input sample dimensions ( $20 \times 2$  - detailed in Section 4.1) using fully padded convolutions.

Table 1: Overall architecture of LEXNet.

Input Dims	Operator	Stride	Out Channels	Cum. Params
$1 \times 20 \times 2$	Conv3x3+BN	1	8	88
$8 \times 20 \times 2$	LERes Block	1	16	3,088
$16 \times 20 \times 2$	LERes Block	1	16	7,760
$16 \times 20 \times 2$	LERes Block	1	32	19,520
$32 \times 20 \times 2$	LERes Block	1	32	38,080
$32 \times 20 \times 2$	LPProto Layer	-	400	50,880
$400 \times 20 \times 2$	Max Pooling	-	400	50,880
$400 \times 1 \times 1$	FC	-	200	130,880

## 4 Evaluation Setting

In this section, we present the methodology employed (dataset, algorithms, hyperparameters and configuration) to evaluate our approach.

### 4.1 Dataset

Our real-world commercial-grade dataset<sup>3</sup> has been collected from four customer deployments in China. The dataset is composed of the TCP (e.g., HTTP) and UDP (e.g., streaming media, VoIP) traffic activity over four weeks across tens of thousands network devices. Specifically, it contains 9.7M flows/MTS belonging to 200 applications/classes (169 TCP and 31 UDP). For each flow/MTS, we have available some per-packet information (two variables: packet size and direction). We set the MTS length to the first 20 packets. This value reflects the relevant time windows to identify the applications and sustain line rate classification of the traffic. Concerning the labeling, each flow has been annotated with application names provided by a commercial-grade deep packet inspection (DPI) engine, i.e. a traditional rule-based method. Traffic encryption in China is not as present as in the Western world yet, so DPI technologies still offer fine-grained view on traffic.

Table 2 presents the structure of the dataset. We observe a class imbalance as the top 10 applications represent more than 40% of the flows. This is characteristic of the traffic classification task and we show in Section 5.1 that our classifier is robust to this class imbalance. Moreover, we can observe that there is no distortion between the proportion of TCP applications (84%) and TCP flows (70-80%).

### 4.2 Algorithms

We compare our algorithm LEXNet to the state-of-the-art classifiers presented in Section 2. Specifically, we used the authors' implementation of CondenseNetV2 [Yang *et al.*, 2021b], MLSTM-FCN [Karim *et al.*, 2019], ProtoPNet [Chen *et al.*, 2019], XCM [Fauvel *et al.*, 2021]. Moreover, we

<sup>3</sup>An anonymized version of our dataset is under preparation for publication.

Table 2: Composition of our dataset. Applications are presented in descending order of their popularity.

Applications	Flows (M)	Flows (%)	TCP %
10	4.1	42.9	70.0
20	5.7	59.4	69.5
50	7.8	80.3	74.5
100	9.0	92.9	76.2
200	9.7	100.0	76.6

used the PyTorch Hub [PyTorch, 2021a]/Torchvision [PyTorch, 2021b] implementations of DenseNet [Huang *et al.*, 2017], EfficientNet [Tan and Le, 2019], GhostNet [Han *et al.*, 2020], MobileNetV3 [Howard *et al.*, 2019], ResNet [He *et al.*, 2016], and ShuffleNetV2 [Ma *et al.*, 2018]. Then, we have implemented with PyTorch in Python 3.6 the 1D CNN, and LEXNet using the public implementations of ProtoPNet [Chen *et al.*, 2019] and ResNet [PyTorch, 2021b]. Finally, we used the public implementations available for ensembles (Random Forest [Pedregosa *et al.*, 2011], XG-Boost [Chen and Guestrin, 2016]) and post-hoc explainability methods (Grad-CAM [Selvaraju *et al.*, 2017], SHAP [Lundberg and Lee, 2017]).

### 4.3 Hyperparameters

Adopting a conservative approach, we performed a 50% train/50% test split of the dataset and preserved the structure of the dataset (train/test split will be made available with dataset release). Hyperparameters have been set by grid search based on the best average accuracy following a stratified 5-fold cross-validation on the training set. As recommended by the authors, we let the number of LSTM cells vary in  $\{8, 64, 128\}$  for MLSTM-FCN, and the size of the window vary in  $\{20\%, 40\%, 60\%, 80\%, 100\%\}$  for XCM. Considering the size of our input data ( $20 \times 2$ ), we let the hyperparameters of ProtoPNet and LEXNet (number and size of the prototypes) vary in  $\{1, 2, 3, 4\}$ . For the other architectures, we use the default parameters suggested by the authors.

### 4.4 Configuration

All the models have been trained with 1000 epochs, a batch size of 1024 and the following computing infrastructure: Ubuntu 20.04 operating system, GPU NVIDIA Tesla V100 with 16GB HBM2. With regard to the limited computational resources of network devices, we also evaluate the models without GPU acceleration on an Intel Xeon Platinum 8164 CPU (2.00GHz, 71.5MB L3 Cache).

## 5 Results and Discussions

In this section, we first present the performance results of LEXNet on the traffic classification task. Then, we discuss the explainability-by-design feature of our approach.

### 5.1 Classification

**CNN Backbone** First, in order to determine the starting architecture for the backbone of LEXNet, we compare the state-of-the-art classifiers. Table 3 presents the accuracy and inference time of the classifiers (with comparable model size around 300k edges - trainable parameters or leafs). This

Table 3: Accuracy and inference time of the state-of-the-art classifiers on the TCP+UDP test set.

Metric	ResNet			1D CNN	Mobile NetV3	Shuffle NetV2	Condense NetV2	Dense Net	MLSTM FCN	XCM	Ghost Net	Efficient Net	RF	XGB
Accuracy (%)	86.7	<b>90.4</b>	89.6	84.5	85.7	86.9	87.9	89.5	86.5	88.1	88.6	86.6	84.4	84.7
$\pm$ 0.2	$\pm$ 0.2	<b><math>\pm</math> 0.1</b>	$\pm$ 0.2	$\pm$ 0.2	$\pm$ 0.3	$\pm$ 0.3	$\pm$ 0.1	$\pm$ 0.4	$\pm$ 0.3	$\pm$ 0.2	$\pm$ 0.3	$\pm$ 0.4	$\pm$ 0.2	$\pm$ 0.2
Inf. GPU ( $\mu$ s/sample)	0.9	1.6	6.1	<b>1.4</b>	2.2	2.5	3.1	3.3	4.6	8.1	11.5	13.3	-	-
Inf. CPU ( $\mu$ s/sample)	16.6	34.6	98.6	<b>26.6</b>	48.6	69.8	80.3	91.8	186.3	355	473.8	610.8	1.6E5	6.2E4
# Edges (k)	138	303	1003	274	312	305	326	328	394	315	322	308	349	352
Mult-Adds (M)	0.5	2.1	20.1	0.6	0.7	0.5	0.4	8.3	2.3	2.6	6.9	2.2	-	-

approach already allows us to reduce the model size by a factor of five compared to the current state-of-the-art traffic classifiers (1-2M of trainable parameters - see Section 2) while maintaining the same level of accuracy (ResNet 138k: 86.7%, 303k: 90.4%, 1M: 89.6% - see left side of Table 3). Then, we observe that the model obtaining the best accuracy on our dataset is ResNet (90.4%), while getting the lowest variability across folds (0.1%). Moreover, ResNet exhibits the best accuracy/inference time trade-off; it obtains the second position with regard to the inference time on both GPU and CPU. Traditional tree-based ensemble methods - Random Forest and XGBoost - obtain an accuracy close to the Vanilla CNN (84.5%), while being around a thousand time slower. Concerning the state-of-the-art efficient CNNs, they all exhibit a higher inference time than ResNet. In particular, some efficient CNNs with really low FLOPs/Multiply-Adds (e.g., CondenseNetV2: 0.4M) compared to ResNet (2.1M) have a much higher inference time (e.g., CondenseNetV2: GPU  $3.1\mu$ s/CPU  $80.3\mu$ s versus GPU  $1.6\mu$ s/CPU  $34.6\mu$ s). The extensive use of operations that reduce the number of FLOPs (e.g., depthwise and 1x1 convolutions) do not translate into reduction in inference time due to factors like memory access cost [Ridnik *et al.*, 2021]. Thus, our experiments show that optimizing FLOPs does not always reflect equivalently into inference time, and emphasize the interest of comparing model performance on the same model size.

Nonetheless, a model is faster than ResNet: the Vanilla 1D CNN (GPU  $1.4\mu$ s/CPU  $26.6\mu$ s versus GPU  $1.6\mu$ s/CPU  $34.6\mu$ s). The absence of residual connection in the 1D CNN can explain this lower inference time. Therefore, we have selected ResNet as starting point for our backbone and worked to reduce its number of weights and inference time by introducing a new residual block (LRes), while maintaining its accuracy as detailed in next section.

**LEXNet versus ProtoPNet** The starting point of our approach, and our state-of-the-art explainable-by-design CNN baseline, is ProtoPNet. Table 4 shows the ablation study from ProtoPNet to LEXNet with our two contributions: a new lightweight and efficient residual block (LRes) and a lightweight prototype layer (LProto). The performances reported correspond to the ones with the best hyperparameter configuration obtained by cross-validation on the training set for both networks: two prototypes of size (1, 1) per class. First, ProtoPNet with ResNet as CNN backbone exhibits an accuracy of 86.2% with 199k trainable parameters. This reduction in model size compared to ResNet (303k parameters - see Table 3) comes from the reduction in size of the fully connected network used for classification (ProtoPNet: 400 values as input - 2 similarity scores/prototypes per

class). Then, we can see that the replacement of the prototype block of ProtoPNet by LProto significantly reduces the number of parameters (-29% of trainable parameters), while increasing the accuracy of the network by 4% to reach 90.4%. As a consequence, the adoption of LProto also leads to a significant reduction in inference time (GPU: -27%/CPU: -17%). Specifically, the reduction of the number of parameters and inference time come from the removal of the convolutional layers, which also decreases the depth of the prototypes. And, the increase in accuracy mainly comes from the L2 regularization (+2.8%) which improves the generalization ability of our approach. Next, the replacement of the original residual block by LRes block allows ResNet to be faster than the Vanilla CNN (GPU  $1.3\mu$ s/CPU  $20.3\mu$ s versus GPU  $1.4\mu$ s/CPU  $26.6\mu$ s), while reducing the number of trainable parameters of its backbone by 19% and maintaining the accuracy (99.3% of the original ResNet). When used in ProtoPNet, we observe in Table 4 a comparable performance evolution as LRes block reduces the backbone parameters and CPU inference time by 19%, while preserving the accuracy (-0.7%). Our LRes block integrates two new operations (generation of cost-efficient feature maps with a linear transformation, concatenation on shortcut connection), and we can observe that both operations reduce the number of trainable parameters and the inference time, with the second operation having twice the impact of the first one. Overall, our explainable-by-design LEXNet is more accurate (+4%), lighter (-34%) and faster (-33%) than the current state-of-the-art explainable-by-design CNN network ProtoPNet, while not inducing a higher variability across folds (0.1%).

Table 4: Ablation study of LEXNet.

	Accuracy (%)	# Params (k)	Inf. GPU ( $\mu$ s/sample)	Inf. CPU ( $\mu$ s/sample)
<b>(0) ProtoPNet</b>	<b>86.2 <math>\pm</math> 0.1</b>	<b>199</b>	<b>5.5</b>	<b>169.7</b>
(1):(0)+No Add. Conv	+0.2	-59	-1.5	-29.3
(2):(1)+Sigmoid	+1.2			-0.6
(3):(2)+L2 Reg	+2.8			+1
<b>(3): (0)+LProto</b>	<b>90.4 <math>\pm</math> 0.1</b>	<b>140</b>	<b>4.0</b>	<b>140.8</b>
Summary	+4%	-29%	-27%	-17%
(4):(3)+Linear Transf.	-0.5	-3	-0.1	-11.9
(5):(4)+Concatenate	-0.2	-6	-0.2	-15
<b>LEXNet: (3)+LRes</b>	<b>89.7 <math>\pm</math> 0.1</b>	<b>131</b>	<b>3.7</b>	<b>113.9</b>
Summary	+4%	-34%	-33%	-33%

**LEXNet Predictions** In this section, we analyze the prediction performance of LEXNet on traffic classification. First, our results show that Internet encrypted flows can be classified with a high state-of-the-art accuracy of 89.7% using solely the values of two prototypes of size (1, 1) per application based on MTS containing the first 20 packets of a

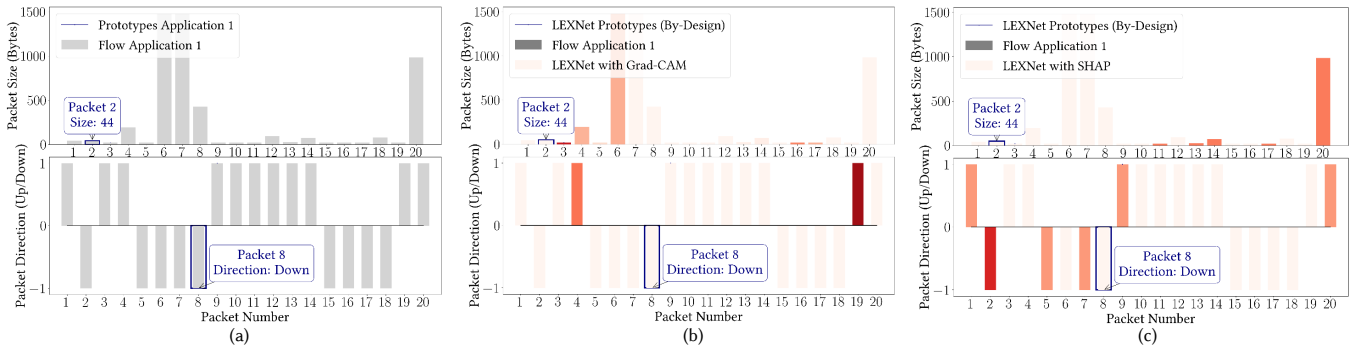


Figure 3: (a) Example of a flow from one popular TCP application of our dataset with the prototypes identified by LEXNet with its explainability-by-design in blue. (b-c) Same flow with the two prototypes identified by LEXNet with its explainability-by-design in blue versus the post hoc explainability methods Grad-CAM (b) and SHAP (c) in red.

flow, with per-packet size and direction as variables. More particularly, two prototypes of size (1, 1) per application are sufficient to classify both TCP and UDP applications with a high state-of-the-art accuracy of 87.8% for TCP and 95.9% for UDP (consistent with [Yang *et al.*, 2021a]). This best hyperparameter configuration (two prototypes of size (1, 1)) also informs us that the information necessary to discriminate applications is often not long sequence of packet sizes or directions, but the combination of both packet sizes and directions at different places of the flow.

Finally, Internet traffic is highly imbalanced, with a few applications generating most of the flows. As an example, half of the classes (100 classes) represent less than 10% of the total number of flows in our dataset (see Table 2). Our results show that, by maintaining the same overall high accuracy as ResNet and a comparable accuracy per class, the addition of a prototype layer for explainability doesn't alter the robustness of our model to class imbalance. Among the 100 less popular classes, more than a third of them are classified with an accuracy above 75%.

## 5.2 Explainability

**Illustration** The explainability of our approach stems from the communication of the two prototypes from the predicted application to the end-user. Based on the first 20 packets of a flow from one popular TCP application, Figure 3a illustrates this explainability by identifying in blue the two class-specific prototypes that have been used for the prediction. The flow is represented with a bar chart for each variable and the two prototypes of size (1, 1) are highlighted by two blue rectangles identifying precisely the region of the input data that has been used for prediction. In this example, a small packet of size 44 in position 2 and a descending packet in position 8 have been detected, which are characteristic of the class containing this popular TCP application. When comparing flows from different applications, this representation allows the end-user/network expert to identify the signature of each application.

**Faithfulness** Then, we highlight the faithfulness of LEXNet explanations, which is critical from both a compliance and business standpoint. We compare the two most important regions of size (1, 1) identified by the faithful (by definition) LEXNet explainability-by-design - the two class prototypes -

to the ones from the state-of-the-art post hoc model-specific method Grad-CAM and model-agnostic method SHAP. First, based on one sample from one popular TCP application, we show in Figure 3b-c that the post hoc explainability methods, applied on the same model LEXNet, identify none of the expected regions/prototypes used by LEXNet. These methods identify regions (in red) which can be far from the expected ones (e.g., Direction: Grad-CAM #19 versus SHAP #2 versus LEXNet #8). Second, in order to quantitatively assess this difference across the dataset, considering that two prototypes need to be identified, we calculate the top-2 and top-10 accuracy in a similar fashion as the top-1 and top-5 accuracies in computer vision evaluations. The results in Table 5 show that Grad-CAM slightly better identifies the regions of the input data that are used by LEXNet (prototypes) compared to SHAP, but overall both post-hoc methods poorly perform (Grad-CAM: top-2 8.7%/top-10 39.9%, SHAP top-2 6.1%/top-10 27.8%). When using the 10 first predicted (1, 1) regions from the post hoc explainability methods, i.e. 25% of the size of the input data, the expected prototypes are identified with an accuracy of less than 40%. Therefore, this experiment clearly emphasizes the importance of adopting explainable-by-design methods compared to post-hoc ones in order to ensure faithfulness.

Table 5: Faithfulness evaluation on the TCP+UDP train set: ability of the state-of-the-art post hoc explainability methods to identify the prototypes used by LEXNet to predict.

LEXNet	By-Design	+ Grad-CAM	+ SHAP
Top-2 Regions Accuracy (%)	100.0	8.7	6.1
Top-10 Regions Accuracy (%)	-	39.9	27.8

**The Cost of Explainability** We have seen that our new CNN LEXNet maintains the same accuracy as the best state-of-the-art neural network on traffic classification (ResNet), while having less than half of its trainable parameters. Moreover, when accounting for explainability, LEXNet also exhibits a lower inference time than ResNet. Table 6 shows the performance of LEXNet (accuracy/size/inference) in comparison with the current state-of-the-art explainable-by-design CNN ProtoPNet with the same backbone as LEXNet, and the best performing CNN (ResNet) which can only rely on state-of-the-art post hoc explainability methods. In addition

to the faithfulness, we observe that LEXNet is around  $2.5\times$  faster than ResNet with LERes block using the most popular post-hoc explainability method for CNNs (the saliency method Grad-CAM), while maintaining the accuracy (89.7%) and halving the model size (131k parameters).

Table 6: Comparison of LEXNet and the state-of-the-art CNNs with explainability-by-design and post-hoc explainability on the TCP+UDP test set.

	Accuracy (%)	# Params (k)	GPU ( $\mu\text{s}/\text{sample}$ )	CPU ( $\mu\text{s}/\text{sample}$ )
ResNet* + Grad-CAM	89.7	294	9.5	278.6
ResNet* + SHAP	89.7	294	8.3E3	6.8E4
ProtoPNet*	86.2	199	5.2	142.8
LEXNet*	<b>89.7</b>	<b>131</b>	<b>3.7</b>	<b>113.9</b>

\*All networks adopt LERes block to keep the same basis of comparison.

Nonetheless, the explainability-by-design of LEXNet has a cost on the inference time compared to the best performing state-of-the-art CNN ResNet without explainability methods (GPU  $3.7\mu\text{s}/\text{sample}$  versus GPU  $1.3\mu\text{s}/\text{sample}$ ). Based on our experiments, around 80% of this additional inference time is due to the L2 distance calculations in the prototype layer to generate the similarity matrices – which thus could benefit some optimization.

## 6 Conclusion

We have presented LEXNet, a new lightweight, efficient and explainable-by-design CNN for traffic classification which relies on a new residual block and prototype layer. LEXNet exhibits a significantly lower model size and inference time compared to the state-of-the-art explainable-by-design CNN ProtoPNet, while being more accurate. Plus, LEXNet is also lighter and faster than the best performing state-of-the-art neural network ResNet with post hoc explainability methods, while maintaining its accuracy. Our results show that Internet encrypted flows can be classified with a high state-of-the-art accuracy using solely the values of two prototypes of size (1, 1) per application based on MTS containing the first 20 packets of a flow, with per-packet size and direction as variables. These two class prototypes detected on a flow can be given to the end-user as a simple and faithful explanation to support LEXNet application prediction.

While LEXNet constitutes a first fruitful attempt to provide faithful explainability for traffic classification with high prediction performance, it could be further improved. For instance, our analysis of LEXNet classification errors reveals that the best hyperparameter configuration on average (two prototypes of size (1, 1)) is not optimal for every applications. The prototype size of (1, 1) offers a high flexibility to cover the needs of different applications. However, the low number of two prototypes per class does not cover applications characterized with more than two values, or applications with a higher diversity of flows. In our future work, we would like to (i) improve LEXNet prediction performance by learning a different number of prototypes per application in order to better characterize the diversity of flows, and (ii) optimize the generation of the similarity matrices in the prototype layer to enhance LEXNet efficiency.

## References

- [Aceto *et al.*, 2019a] G. Aceto, D. Ciuonzo, A. Montieri, and A. Pescape. MIMETIC: Mobile Encrypted Traffic Classification using Multimodal Deep Learning. *Computer Networks*, 165:106944, 2019.
- [Aceto *et al.*, 2019b] G. Aceto, D. Ciuonzo, A. Montieri, and A. Pescape. Mobile Encrypted Traffic Classification Using Deep Learning: Experimental Evaluation, Lessons Learned, and Challenges. *IEEE Transactions on Network and Service Management*, 16(2):445–458, 2019.
- [Aceto *et al.*, 2020] G. Aceto, D. Ciuonzo, A. Montieri, and A. Pescape. Toward Effective Mobile Encrypted Traffic Classification through Deep Learning. *Neurocomputing*, 409:306–315, 2020.
- [Bagnall *et al.*, 2018] A. Bagnall, J. Lines, and E. Keogh. The UEA UCR Time Series Classification Archive. 2018.
- [Baydogan and Runger, 2016] M. Baydogan and G. Runger. Time Series Representation and Similarity Based on Local Autopatterns. *Data Mining and Knowledge Discovery*, 30(2):476–509, 2016.
- [Beliard *et al.*, 2020] C. Beliard, A. Finamore, and D. Rossi. Opening the Deep Pandora Box: Explainable Traffic Classification. In *Proceedings of the IEEE Conference on Computer Communications Workshops*, pages 1292–1293, 2020.
- [Boutaba *et al.*, 2018] R. Boutaba, M. Salahuddin, N. Limmam, S. Ayoubi, N. Shahriar, F. Estrada-Solano, and O. Caceido. A Comprehensive Survey on Machine Learning for Networking: Evolution, Applications and Research Opportunities. *Journal of Internet Services and Applications*, 9(16), 2018.
- [Breiman, 2001] L. Breiman. Random Forests. *Machine Learning*, 45:5–32, 2001.
- [Chen and Guestrin, 2016] T. Chen and C. Guestrin. XG-Boost: A Scalable Tree Boosting System. In *Proceedings of the 22nd ACM SIGKDD International Conference on Knowledge Discovery and Data Mining*, 2016.
- [Chen *et al.*, 2019] C. Chen, O. Li, D. Tao, A. Barnett, C. Rudin, and J. Su. This Looks Like That: Deep Learning for Interpretable Image Recognition. In *Proceedings of the 33rd Conference on Neural Information Processing Systems*, 2019.
- [Chen *et al.*, 2020] Z. Chen, Y. Bei, and C. Rudin. Concept Whitening for Interpretable Image Recognition. *Nature Machine Intelligence*, 2:772–782, 2020.
- [Cisco, 2018] Cisco. Application Visibility and Control User Guide. *Online*, 2018.
- [Crotti *et al.*, 2007] M. Crotti, M. Dusi, F. Gringoli, and L. Salgarelli. Traffic Classification through Simple Statistical Fingerprinting. *ACM SIGCOMM Computer Communication Review*, 37(1):5–16, 2007.
- [Dainotti *et al.*, 2012] A. Dainotti, A. Pescape, and K. Claffy. Issues and Future Directions in Traffic Classification. *IEEE Network*, 26(1):35–40, 2012.

- [Dias *et al.*, 2019] K. Dias, M. Pongelupe, W. Caminhas, and L. de Errico. An Innovative Approach for Real-Time Network Traffic Classification. *Computer Networks*, 158:143–157, 2019.
- [Dignum, 2017] V. Dignum. Responsible Artificial Intelligence: Designing AI for Human Values. *ITU Journal*, 1:1–8, 2017.
- [Du *et al.*, 2020] M. Du, N. Liu, and X. Hu. Techniques for Interpretable Machine Learning. *Communications of the ACM*, 2020.
- [Elsayed *et al.*, 2019] G. Elsayed, S. Kornblith, and Q. Le. Saccader: Improving Accuracy of Hard Attention Models for Vision. In *Proceedings of the 33rd International Conference on Neural Information Processing Systems*, 2019.
- [Fauvel *et al.*, 2020] K. Fauvel, V. Masson, and E. Fromont. A Performance-Explainability Framework to Benchmark Machine Learning Methods: Application to Multivariate Time Series Classifiers. In *Proceedings of the IJCAI-PRICAI Workshop on Explainable Artificial Intelligence*, 2020.
- [Fauvel *et al.*, 2021] K. Fauvel, T. Lin, V. Masson, E. Fromont, and A. Termier. XCM: An Explainable Convolutional Neural Network for Multivariate Time Series Classification. *Mathematics*, 9(23), 2021.
- [Han *et al.*, 2020] K. Han, Y. Wang, Q. Tian, J. Guo, C. Xu, and C. Xu. GhostNet: More Features from Cheap Operations. In *Proceedings of the IEEE Conference on Computer Vision and Pattern Recognition*, 2020.
- [He *et al.*, 2016] K. He, X. Zhang, S. Ren, and J. Sun. Deep Residual Learning for Image Recognition. In *Proceedings of the IEEE Conference on Computer Vision and Pattern Recognition*, 2016.
- [Howard *et al.*, 2019] A. Howard, M. Sandler, B. Chen, W. Wang, L. Chen, M. Tan, G. Chu, V. Vasudevan, Y. Zhu, R. Pang, H. Adam, and Q. Le. Searching for MobileNetV3. In *Proceedings of the IEEE/CVF International Conference on Computer Vision*, 2019.
- [Huang *et al.*, 2017] G. Huang, Z. Liu, L. Van Der Maaten, and K. Weinberger. Densely Connected Convolutional Networks. In *Proceedings of the IEEE Conference on Computer Vision and Pattern Recognition*, 2017.
- [Huawei, 2021] Huawei. Service Awareness. *Online*, 2021.
- [Karim *et al.*, 2019] F. Karim, S. Majumdar, H. Darabi, and S. Harford. Multivariate LSTM-FCNs for Time Series Classification. *Neural Networks*, 116:237–245, 2019.
- [Karlsson *et al.*, 2016] I. Karlsson, P. Papapetrou, and H. Boström. Generalized Random Shapelet Forests. *Data Mining and Knowledge Discovery*, 30(5):1053–1085, 2016.
- [Liu *et al.*, 2019] C. Liu, L He, G. Xiong, Z. Cao, and Z. Li. FS-Net: A Flow Sequence Network for Encrypted Traffic Classification. In *Proceedings of the IEEE Conference on Computer Communications*, pages 1171–1179, 2019.
- [Lotfollahi *et al.*, 2020] M. Lotfollahi, M. Siavoshani, R. Zade, and M. Saberian. Deep Packet: A Novel Approach for Encrypted Traffic Classification Using Deep Learning. *Soft Computing*, 24(3):1999–2012, 2020.
- [Lundberg and Lee, 2017] S. Lundberg and S. Lee. A Unified Approach to Interpreting Model Predictions. In *Proceedings of the 31st International Conference on Neural Information Processing Systems*, 2017.
- [Ma *et al.*, 2018] N. Ma, X. Zhang, H. Zheng, and J. Sun. ShuffleNetV2: Practical Guidelines for Efficient CNN Architecture Design. In *Proceedings of the 14th European Conference on Computer Vision*, 2018.
- [Nascita *et al.*, 2021] A. Nascita, A. Montieri, G. Aceto, D. Ciuonzo, V. Persico, and A. Pescape. XAI Meets Mobile Traffic Classification: Understanding and Improving Multimodal Deep Learning Architectures. *IEEE Transactions on Network and Service Management*, 18(4):4225–4246, 2021.
- [ntop, 2014] ntop. nDPI. *Online*, 2014.
- [Pacheco *et al.*, 2018] F. Pacheco, E. Exposito, M. Gineste, C. Baudoin, and J. Aguilar. Towards the Deployment of Machine Learning Solutions in Network Traffic Classification: A Systematic Survey. *IEEE Communications Surveys & Tutorials*, 21(2):1988–2014, 2018.
- [Parliament and Council, 2021] European Parliament and Council. Artificial Intelligence Act. *European Union Law*, 2021.
- [Pedregosa *et al.*, 2011] F. Pedregosa, G. Varoquaux, A. Gramfort, V. Michel, B. Thirion, O. Grisel, M. Blondel, P. Prettenhofer, R. Weiss, V. Dubourg, J. Vanderplas, A. Passos, D. Cournapeau, M. Brucher, M. Perrot, and E. Duchesnay. Scikit-learn: Machine learning in Python. *Journal of Machine Learning Research*, 12:2825–2830, 2011.
- [Phillips *et al.*, 2021] P. Phillips, C. Hahn, P. Fontana, A. Yates, K. Greene, D. Broniatowski, and M. Przybocski. Four Principles of Explainable Artificial Intelligence. *US National Institute of Standards and Technology*, 2021.
- [PyTorch, 2021a] PyTorch. PyTorch Hub. *Online*, 2021.
- [PyTorch, 2021b] PyTorch. Torchvision v0.11.0. *Online*, 2021.
- [Rezaei *et al.*, 2020] S. Rezaei, B. Kroenke, and X. Liu. Large-Scale Mobile App Identification Using Deep Learning. *IEEE Access*, 8:348–362, 2020.
- [Ridnik *et al.*, 2021] T. Ridnik, H. Lawen, A. Noy, E. Ben, B. Sharir, and I. Friedman. TResNet: High Performance GPU-Dedicated Architecture. In *Proceedings of the IEEE Winter Conference on Applications of Computer Vision*, 2021.
- [Rohde&Schwarz, 2020] Rohde&Schwarz. R&S®PACE 2. *Online*, 2020.
- [Rudin, 2019] C. Rudin. Stop Explaining Black Box Machine Learning Models for High Stakes Decisions and Use Interpretable Models Instead. *Nature Machine Intelligence*, 1:206–215, 2019.

- [Sandler *et al.*, 2018] M. Sandler, A. Howard, M. Zhu, A. Zhmoginov, and L. Chen. MobileNetV2: Inverted Residuals and Linear Bottlenecks. In *Proceedings of the IEEE Conference on Computer Vision and Pattern Recognition*, 2018.
- [Schäfer and Leser, 2017] P. Schäfer and U. Leser. Multivariate Time Series Classification with WEASEL + MUSE. *ArXiv*, 2017.
- [Selvaraju *et al.*, 2017] R. Selvaraju, M. Cogswell, A. Das, R. Vedantam, D. Parikh, and D. Batra. Grad-CAM: Visual Explanations from Deep Networks via Gradient-Based Localization. In *Proceedings of the IEEE International Conference on Computer Vision*, 2017.
- [Seto *et al.*, 2015] S. Seto, W. Zhang, and Y. Zhou. Multivariate Time Series Classification Using Dynamic Time Warping Template Selection for Human Activity Recognition. In *Proceedings of the IEEE Symposium Series on Computational Intelligence*, 2015.
- [Tan and Le, 2019] M. Tan and Q. Le. EfficientNet: Rethinking Model Scaling for Convolutional Neural Networks. In *Proceedings of the 36th International Conference on Machine Learning*, 2019.
- [Tuncel and Baydogan, 2018] K. Tuncel and M. Baydogan. Autoregressive Forests for Multivariate Time Series Modeling. *Pattern Recognition*, 73:202–215, 2018.
- [Valenti *et al.*, 2013] S. Valenti, D. Rossi, A. Dainotti, A. Pescape, A. Finamore, and M. Mellia. *Reviewing Traffic Classification*, pages 123–147. Springer Berlin Heidelberg, 2013.
- [Wang *et al.*, 2020] X. Wang, S. Chen, and J. Su. Automatic mobile app identification from encrypted traffic with hybrid neural networks. *IEEE Access*, 8:182065–182077, 2020.
- [Yang *et al.*, 2021a] L. Yang, F. Alessandro, F. Jun, and D. Rossi. Deep Learning and Zero-Day Traffic Classification: Lessons Learned from a Commercial-Grade Dataset. *IEEE Transactions on Network and Service Management*, 18(4):4103–4118, 2021.
- [Yang *et al.*, 2021b] L. Yang, H. Jiang, R. Cai, Y. Wang, S. Song, G. Huang, and Q. Tian. CondenseNetV2: Sparse Feature Reactivation for Deep Networks. In *Proceedings of the IEEE Conference on Computer Vision and Pattern Recognition*, 2021.
- [Zagoruyko and Komodakis, 2016] S. Zagoruyko and N. Komodakis. Wide Residual Networks. In *Proceedings of the British Machine Vision Conference*, 2016.
- [Zhang *et al.*, 2018] Q. Zhang, Y. Wu, and S. Zhu. Interpretable Convolutional Neural Networks. In *Proceedings of the IEEE Conference on Computer Vision and Pattern Recognition*, 2018.
- [Zhang *et al.*, 2020] X. Zhang, Y. Gao, J. Lin, and C. Lu. TapNet: Multivariate Time Series Classification with Attentional Prototypical Network. In *Proceedings of the 34th AAAI Conference on Artificial Intelligence*, 2020.